

# Calculation of parameters multilayer longitudinal piezoactuator for aerospace

## Abstract

In the work we calculate the parameters multilayer longitudinal piezoactuator for aerospace. The PZT multilayer piezoactuator used in aerospace and nanotechnology for correction form satellite antenna shape, focusing compound telescopes, displacement in scanning microscopy and laser interferometer. For calculation of the parameters multilayer piezoactuator is applied method mathematical physics. The parameters of the PZT multilayer piezoactuator are determined.

**Keywords:** multilayer longitudinal piezoactuator, parameter, aerospace, static and dynamic analysis

Volume 10 Issue 2 - 2026

SM Afonin

National Research University of Electronic Technology, MIET, Moscow, Russia

**Correspondence:** SM Afonin, National Research University of Electronic Technology, MIET, 124498, Moscow, Russia

**Received:** April 28, 2026 | **Published:** June 04, 2026

## Introduction

The multilayer longitudinal piezoactuator is used for aerospace and defence for correction form of satellite antenna shape.<sup>1-24</sup> This multilayer longitudinal piezo actuator is used in compound telescopes for focusing, laser interferometers, satellite control systems and deformable mirrors in the aerospace industry, scanning microscopy and vibration damping.<sup>5-29</sup> The parameters of the PZT multilayer piezoactuator are determined.

## Calculation of parameters multilayer longitudinal piezoactuator

The multilayer longitudinal piezoactuator is the electromechanical device for converting electrical energy into mechanical energy with series mechanical connection of the piezolayers and their electrical parallel connection, with the polarizations of every two adjacent piezolayers in opposite directions.<sup>1-3</sup> The parameters of the multilayer longitudinal piezoactuator are determined by method mathematical physics using the equation reverse piezoeffect and the differential equation or the matrix equation.<sup>5-29</sup> This mathematical model is linearity, without thermal effects, hysteresis, creep. The work develops the analytical model for the multilayer longitudinal piezoactuator for aerospace system.

## Static analysis

For the multilayer longitudinal piezoactuator its equation reverse piezoeffect<sup>1-15</sup> has the form

$$S_3 = d_{33} E_3 + s_{33}^E T_3 \quad (1)$$

Where  $S_3$  - longitudinal strain along axes 3, dimensionless,  $E_3$  - electric field along axes 3, V/m,  $T_3$  - mechanical stress along axes 3, Pa,  $d_{33}$  - longitudinal piezomodule, m/V,  $s_{33}^E$  - the longitudinal elastic compliance at the  $E=\text{const}$ ,  $\text{m}^2/\text{N}$ .

Let us consider the static characteristic the multilayer longitudinal piezoactuator at one fixed face and the voltage control. We have maximum displacement  $\xi_m$  at  $F=0$  and maximum force  $F_m$  at  $\xi=0$  in the form

$$\xi_m = d_{33} n U_m \quad (2)$$

$$F_m = -\frac{d_{33} U_m S_0}{s_{33}^E \delta} \quad (3)$$

For the voltage control the PZT multilayer longitudinal piezoactuator at one fixed face and  $d_{33} = 0.4 \cdot 10^{-9} \text{ m/V}$ ,  $\delta = 6 \cdot 10^{-4} \text{ m}$ ,  $n = 20$ ,  $S_0 = 1.8 \cdot 10^{-4} \text{ m}^2$ ,  $s_{33}^E = 3 \cdot 10^{-11} \text{ m}^2/\text{N}$ ,  $U_m = 100 \text{ V}$  we obtain on Figure 1 the maximum displacement  $\xi_m = 800 \text{ nm}$  and the maximum force  $F_m = 400 \text{ N}$ . The measurements were made on UMM-5 press in the range of working loads under mechanical stresses in the longitudinal piezoactuator up to 100 MPa. The error between the experimental data and calculation results is 10%.

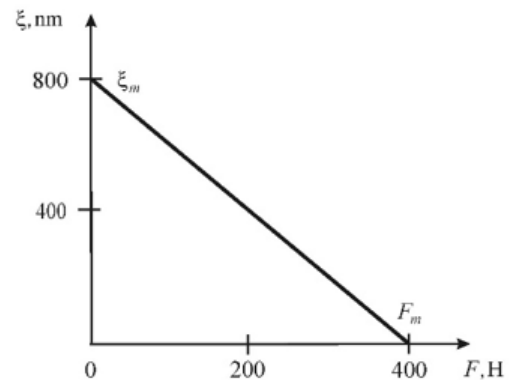


Figure 1 Static characteristic multilayer longitudinal piezoactuator.

## Dynamic analysis

The multilayer longitudinal piezoactuator on Figure 2 consists of piezolayers connected electrically in parallel and mechanically in series.

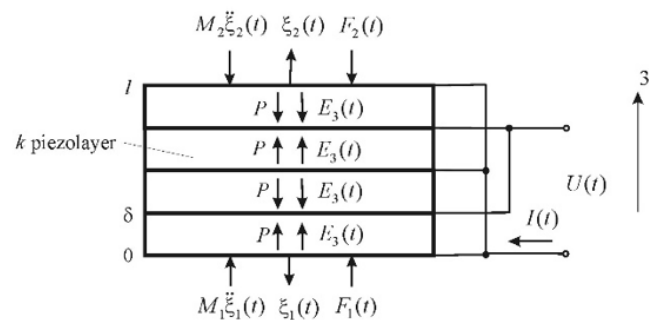


Figure 2 Scheme multilayer longitudinal piezoactuator.

Let us construct the structural model of the multilayer longitudinal piezoactuator. The Laplace transform of the force used for piezoelectric deformation has the form

$$F(p) = \frac{d_{33} S E_3(p)}{s^E} \quad (4)$$

Where  $F(p)$  - Laplace transform force,  $E_3(p)$  - Laplace transform electric field along axes 3,  $p$ - operator.

The circuit of the multilayer longitudinal piezoactuator on Figure 3 is compiled from the equivalent  $T$ -shaped quadripole for  $k$  and  $k+1$  piezolayers

$$F_{k_{inp}}(p) = -(Z_1 + Z_2) \Xi_k(p) + Z_2 \Xi_{k+1}(p) \quad (5)$$

$$-F_{k_{out}}(p) = -Z_2 \Xi_k(p) + (Z_1 + Z_2) \Xi_{k+1}(p) \quad (6)$$

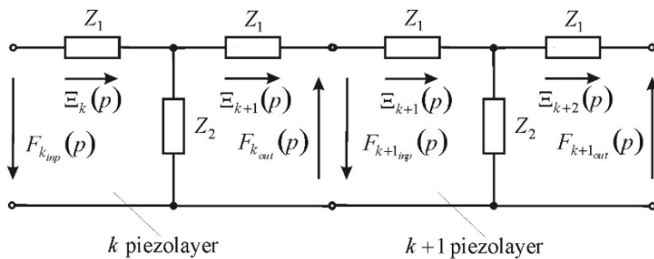


**Figure 3** Circuit multilayer piezoactuator with quadripoles  $k$  and  $k+1$  piezolayers.

Where  $Z_1 = \frac{S_0 \gamma \text{th}(\delta \gamma)}{s^E}$ ,  $Z_2 = \frac{S_0 \gamma}{s^E \text{sh}(\delta \gamma)}$  are the resistance of the

equivalent quadripole of  $k$  piezolayer,  $\delta$  is the thickness of  $k$  piezolayer,  $\gamma = \frac{p}{c^E} + \alpha$  is the coefficient of wave propagation,  $p$  is the operator,

$c^E$  is the speed of sound in the piezoceramics at  $E = \text{const}$ ,  $\alpha$  is the attenuation coefficient,  $F_{k_{inp}}(p)$ ,  $F_{k_{out}}(p)$  are the Laplace transform

of the forces at the input and output ends of  $k$  piezolayer,  $\Xi_k(p)$ ,  $\Xi_{k+1}(p)$  are the Laplace transforms of the displacements at input and output ends of  $k$  piezolayer.

Then we have the Laplace transforms the system of the equations for  $k$  piezolayer on Figure 3 in the form

$$-F_{k_{inp}}(p) = \left(1 + \frac{Z_1}{Z_2}\right) F_{k_{out}}(p) + Z_1 \left(2 + \frac{Z_1}{Z_2}\right) \Xi_{k+1}(p) \quad (7)$$

$$\Xi_k(p) = \frac{1}{Z_1} F_{k_{out}}(p) + \left(1 + \frac{Z_1}{Z_2}\right) \Xi_{k+1}(p) \quad (8)$$

The matrix equation for  $k$  piezolayer

$$\begin{bmatrix} -F_{k_{inp}}(p) \\ \Xi_k(p) \end{bmatrix} = [M] \begin{bmatrix} F_{k_{out}}(p) \\ \Xi_{k+1}(p) \end{bmatrix} \quad (9)$$

And the matrix  $[M]$  in the form

$$[M] = \begin{bmatrix} m_{11} & m_{12} \\ m_{21} & m_{22} \end{bmatrix} = \begin{bmatrix} 1 + \frac{Z_1}{Z_2} & Z_1 \left(2 + \frac{Z_1}{Z_2}\right) \\ \frac{1}{Z_2} & 1 + \frac{Z_1}{Z_2} \end{bmatrix} \quad (10)$$

$$\text{Where } m_{11} = m_{22} = 1 + \frac{Z_1}{Z_2} = \text{ch}(\delta \gamma) \quad (11)$$

$$m_{12} = Z_1 \left(2 + \frac{Z_1}{Z_2}\right) = Z_0 \text{sh}(\delta \gamma) \quad (12)$$

$$m_{21} = \frac{1}{Z_2} = \frac{\text{sh}(\delta \gamma)}{Z_0}, \quad Z_0 = \frac{S_0 \gamma}{s^E} \quad (13)$$

For the multilayer longitudinal piezoactuator of the Laplace transform the displacement  $\Xi_{k+1}(p)$  and the force  $F_{k_{out}}(p)$ , acting on the output face of  $k$  piezolayer on Figure 3, are corresponded to Laplace transforms of displacement and force, acting on the input face of  $k+1$  piezolayer.

The force on the output face for  $k$  piezolayer is equal in amplitude and opposite in direction to the force on the input face for  $k+1$  piezolayer

$$F_{k_{out}}(p) = -F_{k+1_{inp}}(p) \quad (14)$$

The matrix equation for  $n$  piezolayers of the of  $k$  piezolayer has the form:

$$\begin{bmatrix} -F_{k_{inp}}(p) \\ \Xi_1(p) \end{bmatrix} = [M]^n \begin{bmatrix} F_{k_{out}}(p) \\ \Xi_{n+1}(p) \end{bmatrix} \quad (15)$$

With the matrix multilayer longitudinal piezoactuator Figure 3 in the form

$$[M]^n = \begin{bmatrix} \text{ch}(n\delta \gamma) & Z_0 \text{sh}(n\delta \gamma) \\ \frac{\text{sh}(n\delta \gamma)}{Z_0} & \text{ch}(n\delta \gamma) \end{bmatrix} \quad (16)$$

Equations of the forces on two faces of the multilayer longitudinal piezoactuator have the form

$$\text{at } x=0, \quad T_j(0, p) S_0 = F_1(p) + M_1 p^2 \Xi_1(p) \quad (17)$$

$$\text{at } x=l, \quad T_j(l, p) S_0 = -F_2(p) - M_2 p^2 \Xi_2(p) \quad (18)$$

Where  $T_j(0, p)$ ,  $T_j(l, p)$  are the Laplace transforms of mechanical stresses on two faces of the multilayer longitudinal piezoactuator,  $S_0$  is the cross sectional area.

The structural model and the structural scheme on Figure 4 of the multilayer longitudinal piezoactuator at voltage control with  $R = 0$  external circuit resistance and  $l = n\delta$  length actuator are obtained from the equation reverse piezoeffect, the forces on two faces and the system of the equations for the equivalent quadripole of the multilayer longitudinal piezoactuator in the form

$$\Xi_1(p) = \left[ \frac{1}{M_1 p^2} \right] \left\{ -F_1(p) + \left( \frac{1}{\chi_{33}^E} \right) \left[ d_{33} E_3(p) - \left[ \frac{\gamma}{\text{sh}(n\delta\gamma)} \right] \times \right. \right. \\ \left. \left. \times \left[ \text{ch}(n\delta\gamma) \Xi_1(p) - \Xi_2(p) \right] \right] \right\} \quad (19)$$

$$\Xi_2(p) = \left[ \frac{1}{M_2 p^2} \right] \left\{ -F_2(p) + \left( \frac{1}{\chi_{33}^E} \right) \left[ d_{33} E_3(p) - \left[ \frac{\gamma}{\text{sh}(n\delta\gamma)} \right] \times \right. \right. \\ \left. \left. \times \left[ \text{ch}(n\delta\gamma) \Xi_2(p) - \Xi_1(p) \right] \right] \right\} \quad (20)$$

Where  $\chi_{33}^E = s_{33}^E / S_0$ . (21)

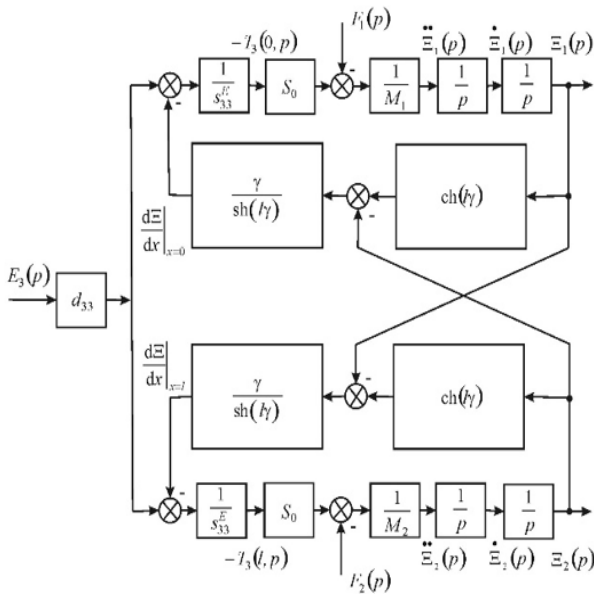


**Figure 4** Structural scheme multilayer longitudinal piezoactuator at voltage control.

**Transfer functions**

Then at the voltage controlled the the multilayer longitudinal piezoactuator we have the transfer functions

$$W_{11}(p) = \Xi_1(p) / E_3(p) = -d_{33} \left[ M_2 \chi_{33}^E p^2 + \gamma \text{th}(n\delta\gamma/2) \right] / A_{ij} \quad (22)$$

$$A_{ij} = M_1 M_2 \left( \chi_{33}^E \right)^2 p^4 + \left\{ \left( M_1 + M_2 \right) \chi_{33}^E / \left[ c^E \text{th}(n\delta\gamma) \right] \right\} p^3 + \\ + \left[ \left( M_1 + M_2 \right) \chi_{33}^E \alpha / \text{th}(n\delta\gamma) + 1 / \left( c^E \right)^2 \right] p^2 + 2\alpha p / c^E + \alpha^2 \quad (23)$$

$$W_{21}(p) = \Xi_2(p) / E_3(p) = d_{33} \left[ M_1 \chi_{33}^E p^2 + \gamma \text{th}(n\delta\gamma/2) \right] / A_{ij} \quad (24)$$

$$W_{12}(p) = \Xi_1(p) / F_1(p) = -\chi_{33}^E \left[ M_2 \chi_{33}^E p^2 + \gamma / \text{th}(n\delta\gamma) \right] / A_{ij} \quad (25)$$

$$W_{13}(p) = \Xi_1(p) / F_2(p) = W_{22}(p) = \Xi_2(p) / F_1(p) = \left[ \chi_{33}^E \gamma / \text{sh}(n\delta\gamma) \right] / A_{ij} \quad (26)$$

$$W_{23}(p) = \Xi_2(p) / F_2(p) = -\chi_{33}^E \left[ M_1 \chi_{33}^E p^2 + \gamma / \text{th}(n\delta\gamma) \right] / A_{ij} \quad (27)$$

For the voltage controlled multilayer longitudinal piezoactuator and the step input voltage  $U_m$  its faces displacements at the inertial load at  $m \ll M_1, m \ll M_2$  and  $F_1(t) = F_2(t) = 0$  have the form

$$\xi_1(\infty) = d_{33} n U_m M_2 / \left( M_1 + M_2 \right) \quad (28)$$

$$\xi_2(\infty) = d_{33} n U_m M_1 / \left( M_1 + M_2 \right) \quad (29)$$

Where  $U_m$  is the amplitude of the voltage,  $m$  is the mass of the multilayer longitudinal piezoactuator,  $M_1, M_2$  are the load masses. For the PZT multilayer longitudinal piezoactuator at  $d_{33} = 4 \cdot 10^{-10}$  m/V,  $n = 8, U_m = 50$  V,  $M_1 = 0.5$  .kg and  $M_2 = 2.5$  kg we obtain the displacements its modules of the faces  $\xi_1(\infty) = 128$  nm,  $\xi_2(\infty) = 32$  nm,

$$\xi_1(\infty) + \xi_2(\infty) = 160 \text{ nm with error } 10\%.$$

**Dynamic characteristic multilayer longitudinal piezoactuator at one fixed face**

The dynamic characteristics of the multilayer longitudinal piezoactuator at one fixed face on Figure 5 are calculated based on the joint solution of the reverse piezoeffect equation and the differential equation.

The equation of forces at the second end on Figure 5 has the form

$$T(l, p) S \Big|_{x=l} = -M p^2 \Xi(p) - C_e \Xi(p) \quad (30)$$

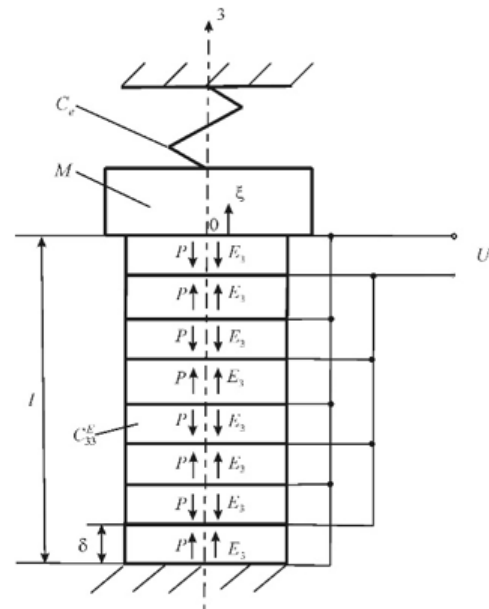


**Figure 5** Scheme multilayer longitudinal piezoactuator at one fixed face and elastic inertial load.

Then from the equation reverse piezoeffect and the equation of forces at the second end we have the equations

$$\frac{d\Xi(x, p)}{dx} \Big|_{x=l} = d_{33} E_3(p) - \frac{s_{33}^E M p^2 \Xi(p)}{S_0} - \frac{s_{33}^E C_e \Xi(p)}{S_0} \quad (31)$$

Then from the differential equation we have equation

$$\frac{\Xi(p)\gamma}{\text{th}(l\gamma)} + \frac{\Xi(p)s^E M p^2}{S_0} + \frac{\Xi(p)s^E C}{S_0} = d_{33} E_3 \quad (32)$$

Then the transfer function for multilayer longitudinal piezoactuator at one fixed face and the elastic inertial load has form

$$W(p) = \frac{\Xi(p)}{U(p)} = \frac{d_{33} n}{M p^2 / C_{33}^E + l\gamma \text{cth}(l\gamma) + C_e / C_{33}^E} \quad (33)$$

After expanding the hyperbolic cotangent into a series, taking into account two terms of the series, we obtain the transfer function in the form

$$W(p) = \frac{\Xi(p)}{U(p)} = \frac{d_{33} n}{\left(1 + C_e / C_{33}^E\right) \left(T_t^2 p^2 + 2T_t \xi_t p + 1\right)} \quad (34)$$

$$T_t = \sqrt{M / \left(C_e + C_{33}^E\right)} \quad (35)$$

Where  $\Xi(p)$ ,  $U(p)$  are the Laplace transforms the displacement face and the voltage,  $T_t$ ,  $\xi_t$  are the time constant and the damping coefficient,  $C_e$  is the rigidity load,  $C_{33}^E$  is the rigidity multilayer longitudinal piezoactuator at  $E=\text{const}$ .

Therefore, its amplitude displacement has the form

$$\xi_m = \frac{d_{33} n U_m}{1 + C_e / C_{33}^E} \quad (36)$$

Where  $\xi_m$  the amplitude displacement and  $U_m$  is the amplitude of the voltage.

In dynamic the expression for the transient response at the voltage control the multilayer longitudinal piezoactuator is determined in the form

$$\xi(t) = \xi_m \left[ 1 - \left( \frac{e^{-\left(\xi_t t / T_t\right)}}{\sqrt{1 - \xi_t^2}} \right) \sin\left(\omega_t t + \phi_t\right) \right] \quad (37)$$

$$\omega_t = \sqrt{1 - \xi_t^2} / T_t, \quad \phi_t = \arctg\left(\sqrt{1 - \xi_t^2} / \xi_t\right) \quad (38)$$

For the voltage control the PZT multilayer longitudinal piezoactuator at one fixed face  $d_{33} = 0.4 \cdot 10^{-9}$  m/V,  $n = 8$ ,  $U_m = 50$  V,  $M = 4$  kg,  $C_{33}^E = 2.3 \cdot 10^7$  N/m,  $C_e = 0.2 \cdot 10^7$  N/m, values the steady state value of displacement face  $\xi_m = 147.2$  nm and the time constant  $T_t = 0.4 \cdot 10^{-3}$  s are obtained with error 10%.

## Discussion

The parameters of the multilayer longitudinal piezoactuator are determined by method mathematical physics using the equation reverse piezoeffect and the differential equation or the matrix equation. The mathematical model in the work is linearity, without thermal effects, hysteresis, creep. This work develops the analytical model for the multilayer longitudinal piezoactuator for aerospace system.

The parameters of multilayer longitudinal piezoactuator with one end fixed are determined for aerospace. Method mathematical physics is used for calculation the parameters of the multilayer longitudinal piezoactuator.

## Conclusion

The multilayer piezoactuator used in aerospace and nanotechnology for correction form satellite antenna shape, focusing compound telescopes, displacement in scanning microscopy and laser interferometer. For calculation of the parameters multilayer piezoactuator is applied method mathematical physics. The parameters of the PZT multilayer piezoactuator are determined. The parameters of the PZT multilayer longitudinal piezoactuator are calculated for aerospace. The transfer functions and its parameters of the PZT multilayer longitudinal piezoactuators are obtained. The transfer functions and dynamic characteristic of the PZT multilayer longitudinal piezoactuator at one fixed face are calculated.

## Acknowledgements

None.

## Conflicts of interest

The author declares that there are no conflicts of interest.

## Funding

None.

## References

- Zhou X, Wu S, Wang X, et al. Review on piezoelectric actuators: materials, classifications, applications, and recent trends. *Front Mech Eng.* 2024;19(1):6.
- Afonin SM. Absolute stability conditions for a system controlling the deformation of an electromagnetoelastic transducer. *Dokl Math.* 2006;74(3):943–948.
- Uchino K. *Piezoelectric Actuator and Ultrasonic Motors*. Boston, MA: Kluwer Academic Publishers; 1997.
- Sun P, Xu Z, Jin L, et al. A novel piezo inertia actuator utilizing the transverse motion of two parallel leaf-springs. *Micromachines (Basel)*. 2023;14(5):954.
- Afonin SM. Solution of the wave equation for the control of an electromagnetoelastic transducer. *Dokl Math.* 2006;73(2):307–313.
- Afonin SM. Erratum to: Solution of the wave equation for the control of an electromagnetoelastic transducer. *Dokl Math.* 2025.
- Cady WG. *Piezoelectricity: An Introduction to the Theory and Applications of Electromechanical Phenomena in Crystals*. New York, NY: McGraw-Hill Book Co; 1946.
- Mason W, ed. *Physical Acoustics: Principles and Methods*. Vol 1, Part A. New York, NY: Academic Press; 1964.
- Zhao C, Li Z, Xu F, et al. Design of a novel three-degree-of-freedom piezoelectric-driven micro-positioning platform with compact structure. *Actuators*. 2024;13(7):248.
- Zwillinger D. *Handbook of Differential Equations*. Boston, MA: Academic Press; 1989.
- Afonin SM. Structural-parametric model and transfer functions of electroelastic actuator for nano- and microdisplacement. In: Parinov IA, ed. *Piezoelectrics and Nanomaterials: Fundamentals, Developments and Applications*. New York, NY: Nova Science Publishers; 2015:225–242.

12. Afonin SM. Structural scheme of electroelastic engine micro and nano displacement for applied bionics and biomechanics. *MOJ Appl Bion Biomech.* 2025;9(1):1–4.
13. Chang Q, Chen W, Zhang S, et al. Review on multiple-degree-of-freedom cross-scale piezoelectric actuation technology. *Adv Intell Syst.* 2024;6:2300780.
14. Afonin SM. Structural-parametric model of electromagnetoelastic actuator for nanomechanics. *Actuators.* 2018;7(1):6.
15. Afonin SM. Structural-parametric model and diagram of a multilayer electromagnetoelastic actuator for nanomechanics. *Actuators.* 2019;8(3):52.
16. Afonin SM. Optimal control of a multilayer electroelastic engine with a longitudinal piezoeffect for nanomechatronics systems. *Appl Syst Innov.* 2020;3(4):53.
17. Afonin SM. Coded control of a sectional electroelastic engine for nanomechatronics systems. *Appl Syst Innov.* 2021;4(3):47.
18. Afonin SM. Structural-parametric model electroelastic actuator nano- and microdisplacement of mechatronics systems for nanotechnology and ecology research. *MOJ Ecol Environ Sci.* 2018;3(5):306–309.
19. Afonin SM. Deformation of electromagnetoelastic actuator for nano robotics system. *Int Robot Autom J.* 2020;6(2):84–86.
20. Afonin SM. Piezo actuators for nanomedicine research. *MOJ Appl Bion Biomech.* 2019;3(2):56–57.
21. Afonin SM. Structural scheme of electromagnetoelastic actuator for nano biomechanics. *MOJ Appl Bion Biomech.* 2021;5(2):36–39.
22. Afonin SM. DAC electro elastic engine for nanomedicine. *MOJ Appl Bion Biomech.* 2024;8(1):38–40.
23. Afonin SM. Multilayer and sectional nano piezo engine for applied bionics and biomechanics. *MOJ Appl Bion Biomech.* 2025;9(1):59–62.
24. Shevtsov SN, Soloviev AN, Parinov IA, et al. *Piezoelectric Actuators and Generators for Energy Harvesting: Research and Development.* Cham, Switzerland: Springer; 2018.
25. Akpinar M, Uzun B, Yayli MO. Dynamics of a piezoelectric restrained nanowire in an elastic matrix. *Mech Solids.* 2024;59(5):2936–2959.
26. Nalwa HS, ed. *Encyclopedia of Nanoscience and Nanotechnology.* Vols 1-25. Valencia, CA: American Scientific Publishers; 2019.
27. Afonin SM. Structural-parametric model of a piezoactuator for nanoscience and nanotechnology. *Eur J Appl Sci.* 2021;9(3):26–36.
28. Afonin SM. Step piezoengine for nano and micro bionics. *MOJ Appl Bion Biomech.* 2026;10(1):22–24.
29. Afonin SM. Calculation of structural scheme nano piezoengine with lumped parameters at voltage and current control for aerospace. *Aeronaut Aerosp Open Access J.* 2025;9(2):113–116.